British Journal of Applied Science & Technology
9(1): 19-36, 2015, Article no.BJAST.2015.243
ISSN: 2231-0843

SCIENCEDOMAIN *international*
www.sciencedomain.org

Chemical and Mineralogical Characterization of Clayey Deposits for Traditional Pottery and Brickworks in the North West Region of Cameroon (Central Africa)

S. L. Wouatong Armand[1*], Tchounang Kouonang Serge[1,2], Hawa Mohamed[2], Yerima K. P. Bernard[3], Melo Chinje Uphie[2] and Njopwouo Daniel[4]

[1]Department of Earth Sciences, Faculty of Science, University of Dschang, P.O.Box 67 Dschang, Cameroon.
[2]Local Materials Promotion Authority (MIPROMALO), Ministry of Scientific Research and Innovation, Yaounde, P.O.Box 2396 Yaounde, Cameroon.
[3]Department of Soil Sciences, Faculty of Agronomy and Agricultural Sciences, University of Dschang, P.O.Box 222 Dschang Cameroon.
[4]Department of Inorganic Chemistry, Faculty of Science, University of Yaounde I, P.O.Box 812, Cameroon.

Authors' contributions

This work was carried out in collaboration of all authors. Authors SLWA and TKS designed the study, performed the characterization of natural clay, wrote the protocol, and wrote the first draft of the manuscript. Author HM managed literature searches under the guidance of authors MCU and ND. Authors MCU and ND managed the analyses of the study (XRD, DTA and TGA). Author YKPB manage the XRD and SEM analyses and corrected the first draft and last version. All authors read and approved the final manuscript.

Article Information

DOI: 10.9734/BJAST/2015/16217
Editor(s):
(1) Grzegorz Zboiński, Institute of Fluid Flow Machinery, Polish Academy of Sciences, Poland.
Reviewers:
(1) Anonymous, Turkey.
(2) Anonymous, Nigeria.
(3) Anonymous, Malaysia.
Complete Peer review History: http://www.sciencedomain.org/review-history.php?iid=1136&id=5&aid=9158

Original Research Article

Received 16th January 2015
Accepted 12th March 2015
Published 8th May 2015

**Corresponding author: E-mail: aslwouat@yahoo.com;*

ABSTRACT

Prospection and characterization studies carried out in the Bamessing area (Nord-West region of Cameroon) has revealed the presence of heterogeneous clayey materials along the lower slopes of Sabga Hill (1240-1320 m altitude) and the upper limits of Ndop plain (approximately 1200 m altitude). Clayey materials identified are dark-grey (on the hill), grey (within the plain) and yellowish (on both the hill and the plain) in color. Raw materials were deposited in the Pan African base. The major phases are kaolinite, illite, hydroxyl-interlayered Na-smectite, chlorite, quartz, gibbsite and goethite. The main clay minerals are composed of kaolinite, illite, hydroxyl-interlayered smectite and chlorite. The whole-rock chemical composition is characterized by silica (< 47 to 66% SiO_2), alumina (15 to 20% Al_2O_3) and iron (3 to 5% Fe_2O_3). Mineralogical and geochemical properties of the materials presented and discussed in this work indicate that the clayey materials of the Bamessing area have a good potential for manufacture of pottery, bricks and tiles.

Keywords: Clayey materials; kaolinite; illite; hydroxyl-interlayered Na-smectite; chlorite Bamessing; Ndop-plain; Cameroon.

1. INTRODUCTION

Nowadays, many scientific works [1-5] have shown the many virtues of clayey materials such as ceramics, medicine, stationery, environment, agronomy, etc. However, in Cameroon, research effort aimed to the prospection, characterization and valorization of clay mineral deposits are still in process. Since time memorial, Man has used these materials for the fabrication of household and artistic objects and for construction works [6,4]. The use of these objects (household, artistic objects and construction works) is on the increase [7,8]. Large areas containing clay mineral deposits are reported in Cameroon, but their mineralogical and chemical characterization is still to be done [9]. This is the case of the Bamessing locality where the local population is actively involved in traditional pottery and the fabrication of fired bricks through the exploitation of clayey deposits. These materials could be economically exploited today but the lack of scientific data on the subject makes it difficult. The present study focuses on the geomorphological, geological, mineralogical and chemical characterization of Bamessing clay deposits, exploited for traditional pottery and the fabrication of fired bricks. The results of this study will give the scientific data such as clay mineralogy and chemistry indispensable for the potential economic exploitation.

2. NATURAL SITE AND GEOLOGICAL SCOPE

The Bamessing locality is situated east of the town of Bamenda and extends from latitude 5°57' to 6°01' North and from longitude 10°20' to 10°25' East (Fig. 1), in Ngoketunjia Division, the Nord-West Region of Cameroon. It has an area of 54,625 km² with an average altitude of 1350 m above sea level.

The hydrographic network shows the subparallel to subdenditic drainage pattern as not being particularly dissected (Figs. 1 and 2).

Generally, the vegetation of the study area presents varying species which reflect the geomorphology of the site.

In the North-Eastern part of the Ndop plain, where the average altitude is 1200 m the vegetation is essentially anthropic, made up of both indigenous farms (subsistence agriculture that produces foods such as, maize, cocoyam, banana, plantain, etc.) and farms of the organization specialized in the cultivation of rice [10]. Equally, isolated clumps of *Cyathae manniana* are obtained in the area. The 1240 to 1340 m altitude zone is essentially dedicated to livestock production and the exploitation of clay. Towards the hilltops the dominant vegetation is as follows:

- Along water-courses, *Raphia venefera* bordered by *Cyathae manniana.* These species witness the regression linked to the exploitation of clay used for pottery and brickworks by the local population, and for commercialisation in the national and international markets. This activity (exploitation of clayey materials) is by far the most important. Along the slope and on the hilltops, *Albizzia gunifera* and *Imperata cylindrica* are reported respectively; these two species serve as pasture for the raring

of cattle. The upper part (above 1450 m altitude), covered with rocky pavement stones is essentially colonized by *Imperata cylindrical*.

- The alluvial soils are dominated by clay in the plain. They are surrounded by lateritic soil of a considerable thickness that vary from a few centimetres to over 8 metres. This alluvium overlies a layer of clay found along the main water-courses. Due to tectonic movement, visible fractures exist that house the water-courses which have same direction. These fractures are of variable importance, and predominate in the N125°E, N140°E and N145°E directions. The area is made up of rock pedestals (plutono-metamorphic) with volcanic rocks and alluvium overlying on top of it (Fig. 2).

The basement rocks are made up of plutonic and metamorphic formations composed of granites, schists and amphibolites, outcropping as vents along the water-courses or on the flanks of the mountain. This basement rocks is the Pan-African [11-14] on which Bamenda mountains rest. The other rock formations are made up of trachytes, benmorites, alkaline to perialkaline rhyolites and basalts [15-17]. Trachytes appear exclusively at the mountain peaks [10]. This rock, occurring in form of slabs and is greenish, massive and encloses laths of feldspar oriented in the same direction as the typical trachytic structure.

The basalts are found within the water-courses and are enclosed by solified volcanic ash [10]. The forms are blackish in color whith the prismatic structure being penta- to hexagonal in shape. The mineralogy of basalts is made up of olivine phenocrysts and pyroxene, present in a massive structure with a microlitic porphyric texture and yellow weathering bands.

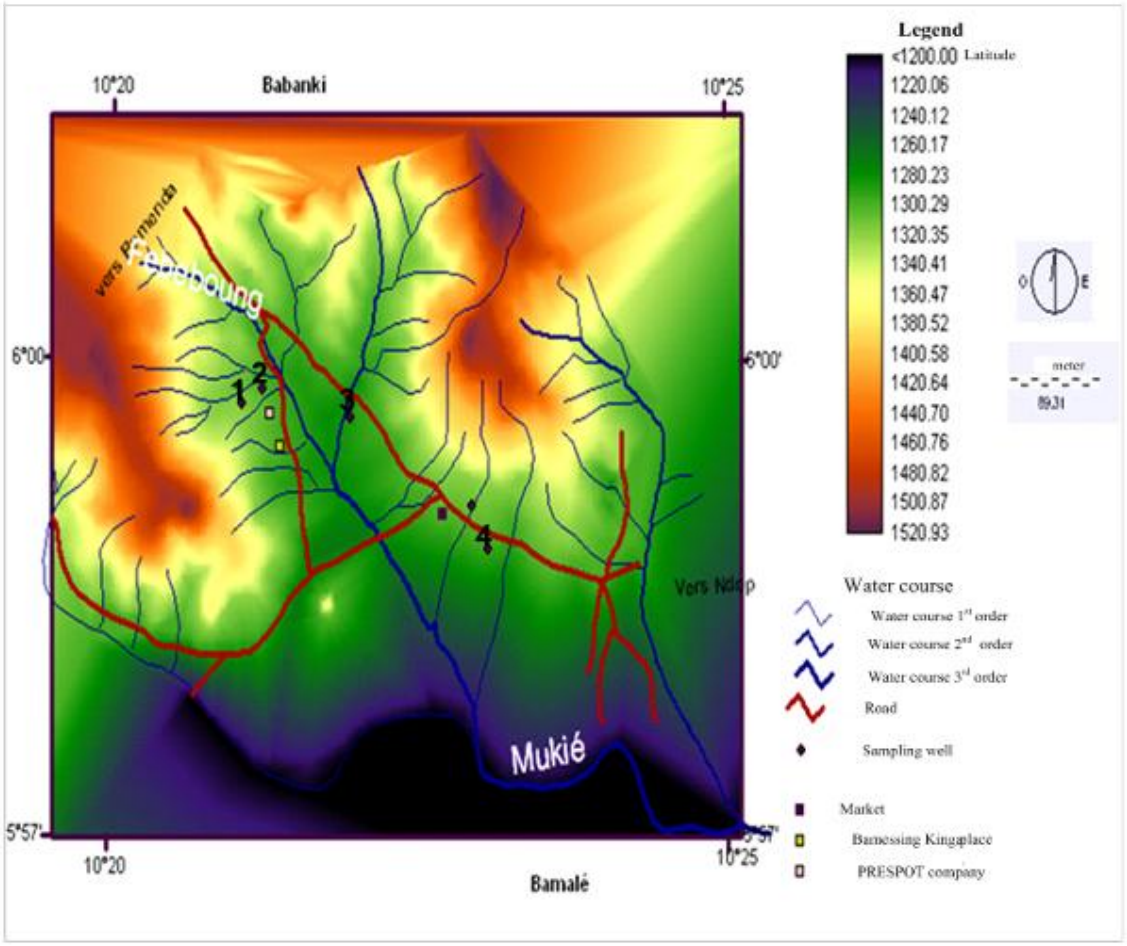

Fig. 1. Map of localization of the study region (extract *from Nkambe 1b* and *Bafoussam 3d*)

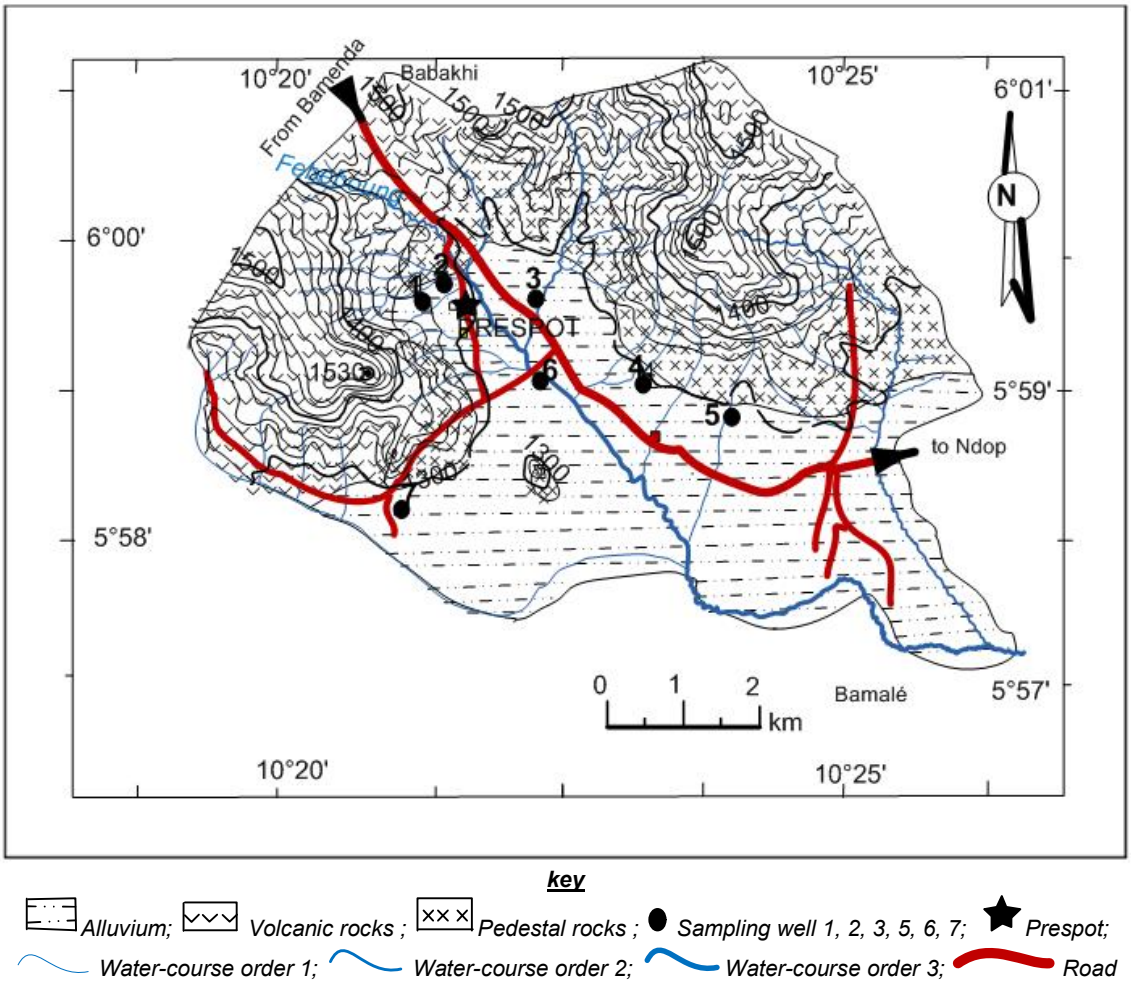

Fig. 2. Stretch of the geological and Hydrographic map of the Bammessing locality [10]

3. MATERIALS AND METHODS

Five wells were dug in the Bamessing locality about 600 m from" PRESPOT" (artisanal clayey materials quarry), along the Mount Sabga Ndop plain axis (Figs. 1, 2). The first well is at 1199 m altitude and is 4 m deep. The second well is at 1196 m altitude and is 6.5 m deep. The third and fourth wells located in the plain are at 1169 m altitude and are 7 and 7.5 m deep, respectively. The fifth is at 1208 m altitude and is 3.15 m deep. From these wells, four specimens 20 to 30 kg each (T1, T2, T6 and T7), representing the specimens from levels II and III from the well 1 and 2 (Figs. 3, 4). The samples were obtained in the profiles described from wells 1 and 2 (selected as representative profiles; dug in Bamessing artisanal quarries). Specimens were selected on the basis of their colors (yellowish, greyish and black colors). T1 and T2 specimens are the main samples used to pottery and will be subject to characterization. On the other sideT6 and T7 specimemens are the new samples from which we just need to know the chemical and mineralogy composition for possible exploitation. Profiles of wells 1 and 3 are alike and differ from those of wells 2, 4 and 5 which are alike. These materials have, pH value between 4.94 to 5.36 and organic content ranging between 2.30 to 5.36% [10].

3.1 Morpho-structural Description of Profiles 1 and 2 and Preparation of Samples

3.1.1 Profile 1

The profile I (Fig. 3) is found at an altitude of 1199 m and has the following characteristics:

- Level 1 (0–60 cm): dark reddish (10R2.5/1); salty-clayey texture; lumpy structure, consistent (humid); porous; few roots; slightly sticky, very less plastic; diffuse boundary.
- Level 2 (60–238 cm): reddish yellow (7.5YR 7/6); clayey-silty-sandy texture; massive structure; consistent (humid); very few roots; sticky; plastic; abrupt boundary. This layer from which T7 specimen was taken is very much solicited by the population to make sun-dry bricks.
- Level 3:

• First upper layer (238–386 cm): black (7.5YR2 5/1); clayey texture; very massive to compact structure; clayey humid, very plastic, sticky; distinct boundary. This layer from which T1 specimen was obtained is so much solicited by the population for pottery.
• Second layer: 386–406 cm; dark grey (2.5Y 4/1); sandy; very soft structure; not compact (humid); not sticky; not plastic; distinct boundary.
• Third layer (406–436 cm): dark greyish brown (10Y 4/2); clayey-sandy texture; massive structure; humid; presence of whitish marks filled with quartz; sticky and plastic; presence of muscovite flakes.

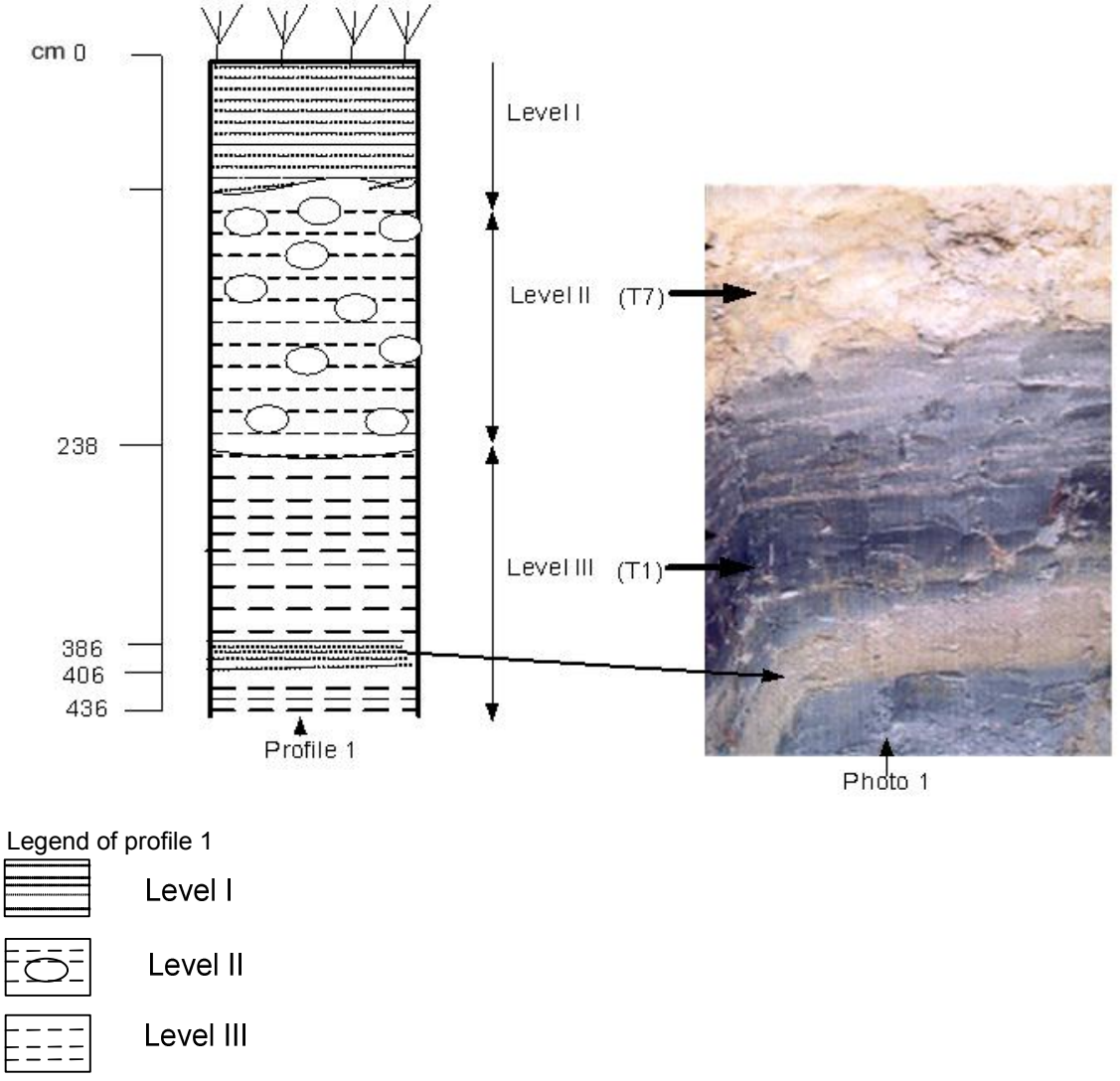

Fig. 3. Profile and photo of profile 1 showing the disposition of different layers [10]

3.1.2 Profile 2

This profile (Fig. 4) from which T6 sample was sampled is located at an altitude of 1196 m and has the following characteristics:

- Level 1 (0–115 cm) : red (2.5YR 4/6), sandy-silty texture, lumpy structure, less compact (humid), very porous, weakly rooted, slightly sticky and slightly plastic, presence of fine gravel 1-10 mm in diameter, brown or rusty marks, irregular boundary.
- Level 2;
  - Upper layer (115–310 cm): reddish yellow (7.5YR 7/6), sandy-silty-clayey texture, very massive structure, modestly consistent, (humid), few pores, very few roots, modestly sticky, few plastic, presence of brown and rusty marks, fragments of pegmatite, diffuse boundary.
  - Bottom layer (310-550 cm): greyish dark brown (10YR 4/2), clayey- sandy texture, massive structure, poorly consistent (humid), few pores, and plastic presence of fragments of pegmatite and marks of rust.
- Level 3 (550-650 cm): dark grey (2.5Y 4/1); clayey-sandy texture; massive structure; humid; few porous very plastic. The materials of this layer, from where the T2 sample was collected are very much in demand by the population for pottery production.

3.2 DTA, TGA, XRD, XRF and SEM Analyses

Analytical techniques used in the study comprise the following (1) thermogravimetric analyses (TGA), (2) differential thermal analyses (DTA), (3) X-ray diffractometry (XRD), (4) scanning electron microscopy (SEM) and (5) X-ray florescence whole-rock chemistry (XRF). The analyses were carried out at the University of Limoges, French (T1 and T2) and at University of Hiroshima, Japan (T6 and T7).

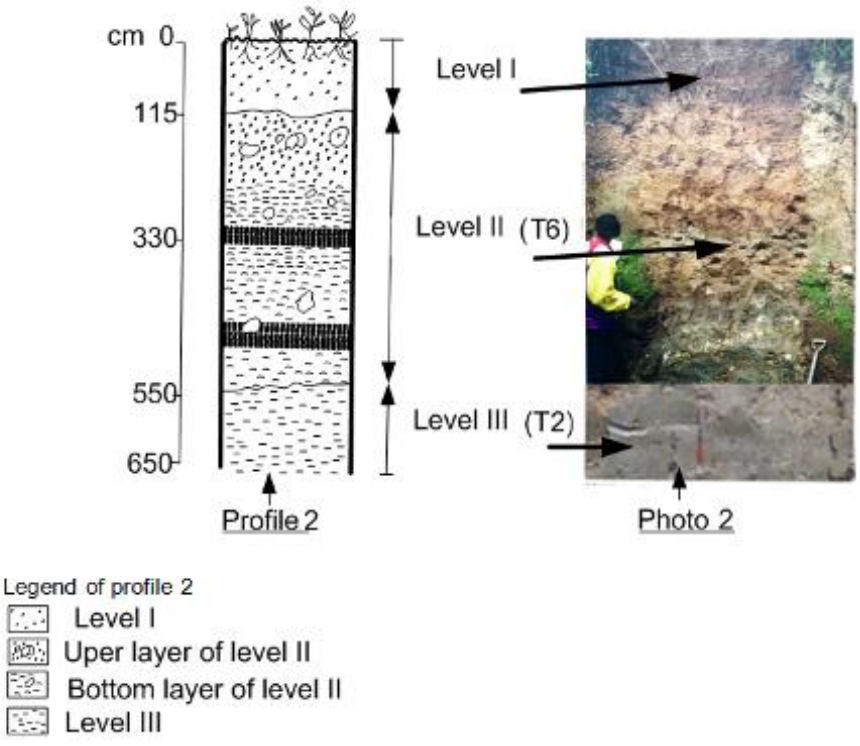

Fig. 4. Profile 2 and photo 2 showing the arrangements of different layers [10]

TGA and DTA analyses permitted us to detect, follow and identify the different thermo-chemical transformations/degradations of the study sample in response to a progressive temperature increase ranging from RT to 1000°C. The TGA and DTA thermograms were obtained under ambient atmosphere. The heating of clayey products resulted in the elimination of organic matter and the escape of water molecules from each of the minerals within the corresponding temperature range and proportions [18]. The influence of temperature enables us to follow up the weight variations of the samples in the course of heating. The differential thermal analysis is done on the coarse and fine soil fractions using 10 and 15 mg of samples, putting them in a platinum micro-melting crucible. Loss in weight of both the sample holder and the sample (micro-melting crucible and fine of coarse fractions) was followed up in an oven in a range between room temperature and 1000°C. The measurements of the TGA were taken on a LINSEIS L70 apparatus. The rise of temperature was constant and equal to 10°C/min for T1 and T2 and 20°C/min for T7. The specimens and calcinated aluminium, used as a standard, were placed into two platinum melting crucibles. These analyses have done with T1, T2 and T7 samples.

For sample T6 the concern emerged about the feldspar presence since a fragment of pegmatite and marks of rust were reported.

Mineral contents of all samples analysed were determined by means of X-ray power diffractions analysis. The measurements were conducted on global samples as well as those treated by formamide (T6 and T7), ethylene glycol (T1 and T2), and heated for one hour to 500°C (T6 and T7) and 550°C (T1 and T2). The X-ray diffraction spectra were acquired both on unoriented powder and on oriented aggregates, according to the methods described in Moore and Reynolds (1989). A Brucker D8-Adance diffractometer device was used and equipped with an INEL CPS 120-Curved position Sensitive Detector was used. This geometry enables the aquisition of diffractograms under a fixed incidence. The CuK & source was used (I = 30 mA, V = 40 kV) along with the dissymmetric graphic monochromator. The measurement were carried out in the 2Θ range from 2º to 40º (T1 and T2) and 2º to 50º (T6 and T7) with step size of 0.02º per 2s step. Interpretation of mineral phases was carried out by using Eva software.

A model FEG-ESEM XL3 scanning electron microscopy was used to observe the morphology and size of kaolinite, illite and quartz minerals in the clay size fraction for samples T1 and T2. The images were obtained by a secondary electron detector after the samples were coating with gold for a accelerating voltaged (10 kV and 15 kV). SEM (CAMBRIDGE mark microscope under operating conditions of 3.0 KV) enabled complete identification of mineral. The clay specimens were there up on put in the acetone suspension. A drop of sample was pipette into the slide, dried and coated.

The concentrations of the major elements of samples T1, T2, T6 and T7 were obtained on a BRUKER (S4 PIONER) wave lengths dispersive (WD-XRF) spectrometer. The powder samples were mixed with 2 g of cellulosic WAX and then pressed in aluminium capsules of 40 mm diameter and 7 mm thickness. A specific standard was developed in order to optimise the WD-XRF for the matrices of specimens to be analysed. This was done using fourteen materials of certified reference, made up of rocks, soils, marine and river sediments, clay, limestone, bauxite with the following codes: NCS DC18009NCS, HCI18802, and CRM N °3193-89, MARL MV, AMIS 0103, AMIS 0110, AMIS 0078, AMIS 0112, AMIS 0076, AMIS 0111, AMIS 0100, AMIS 080, AMIS 0133 and AMIS 0133.The range of elements obtained is the major element and the accuracy is 0.1 ppm.

4. RESULTS

4.1 Thermogravimetry (TGA)

Thermogravimetric analyses of samples T1, T2, T7 are presented in Fig.7 and Table 2.

The thermogravimetric weight loss evolution curves for T1 and T2 (Fig. 5) show three events with the sharp decreases in weight. Two of these are followed by the progressive weight decreases (Table 2). The results of thermogravimetric analyses of the T7 sample show a thermogravimetric evolution curve of weight loss (Fig. 5), with two levels of sharp weight decreases and two levels of progressive weight decreases (Table 1). These variations are represented in Table 1 with the corresponding losses in weight.

4.2 Differential Thermal Analysis (DTA)

The DTA cuves (Fig. 6) present five endothermic peaks for each of the T1 and T2 samples and two endothermic peaks for the T7 sample.

Table 2 shows the different temperature of the samples analysed.

4.3 X-ray Diffraction (XRD) Analysis

The X-ray diffractograms of samples T1, T2, T6 and T7 are presented in Figs. 7, 8, 9 and 10.

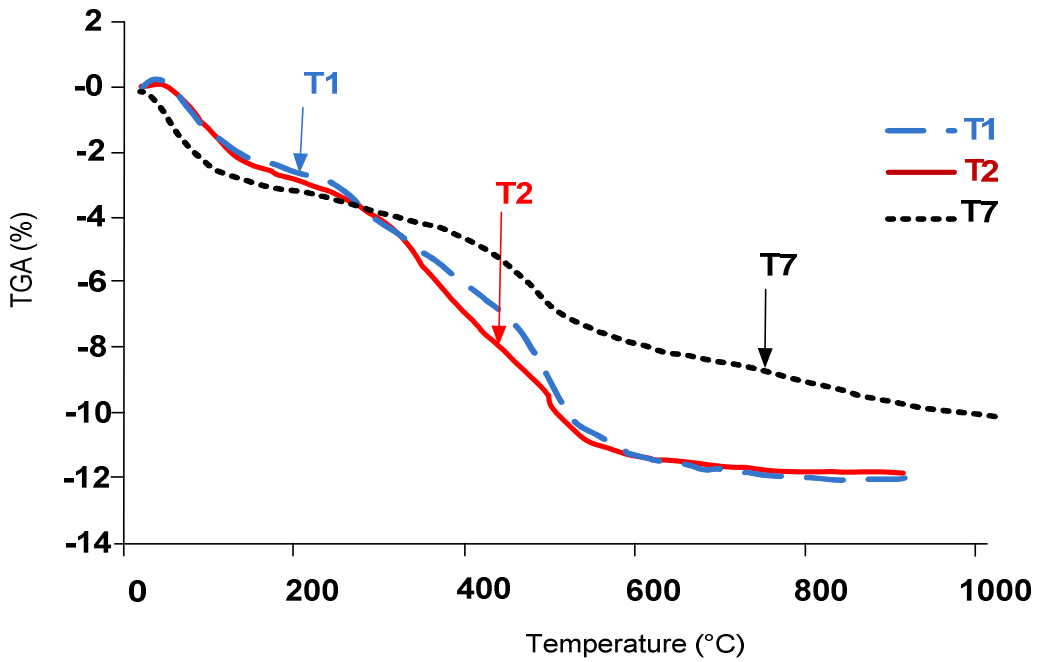

Fig. 5. Thermogravimetric curves for samples T1, T2 and T7

Table 1. Temperatures of the different stages of weight loss

Samples	Designation	Temperature (in °C) at which weight loss is sharp			Temperature (in °C) at which weight loss is progressive	
		First level	Second level	Third level	First level	Second level
T1	Starting temperature	22	200	300	100	659
	Final temperature	100	300	659	200	914
	Weight loss (Percentage of weight loss)	1.25	1.28	6.60	1.04	0.44
T2	Starting temperature	22.57	197.79	300.03	99.79	575.59
	Final temperature	99.79	300.03	575.59	197.04	914.37
	Weight loss (Percentage of weight loss)	2.87	2.65	15.06	3.02	1.52
T7	Starting temperature	24.7	-	307	100.3	550
	Final temperature	100.3	-	550	307	999.8
	Weight loss (Percentage of weight loss)	3.86	-	6.05	2.75	2.76

Table 2. Maximum temperatures of observed endothermic and exothermic peaks on the DTA curves of T1, T2 and T7 samples

Samples	Temperatures of the different endothermic peaks (in °C)						Temperature of the different exothermic peaks	
	1st peak	2nd peak	3rd peak	4th peak	5th peak	6th peak	1st peak	2nd peak
T1 (10°C/min)	74.89	178.44	259.47	498.25	557.41	-	339.03	-
T2 (10°C/min)	67.05	171.36	264.11	503.67	553.63	733.65	350.57	-
T7 (20°C/min)	76.7	-	253.1	477.6	567	810	20	941.1

These diffractograms (Figs. 7, 8, 9 and 10) show similar mineral phases.

- Kaolinite is characterised by the peaks at 2Θ: 12.48° and 24.6°, respectively corresponding to d (001) = 7.19 Å and d (002) = 3.58 Å. Illite is characterised by peaks at 2Θ: 8.84°, 16.38° and 26.60° corresponding to d (002) = 10.32 Å, d (004) =5.40 Å and d (006) = 3.36 Å. Gibbsite is characterised by the peak at 2Θ = 18.2° corresponding to d (002) = 4.85 Å, and goethite is characterised by the peak at 2Θ = 21.23° corresponding to d(100)= 4.18 Å. Quartz is characterised by peaks at 2Θ : 20.50°and 26.06° corresponding to d(100) = 4.26 Å and d (011) = 3.34 Å respectively. Chlorite is characterised by peak at 2Θ = 6° corresponding to d (001) = 14.28 Å. Hydroxyl-interlayered smectite (HIS) are characterised by 2Θ = 8.2° corresponding to d (001) = 12.26 Å and 12.48 Å respectivelly in untreated and treated with formamide or ethylene glycol sample.

4.4 Scanning Electron Microscopy (SEM)

The SEM observations show scattered piles of kaolinites (Figs 11a and 11b), illite (Fig. 11a) and of quartz (Fig. 11b) with irregular shape. The etch pit depicted in photo 4 is analogue to those observed in nature and experimentally on quartz grains by previous investigations [19,20].

4.5 Chemical Composition of Clay Materials

Table 3 presents the chemical composition of samples T1, T2, T6 and T7. The chemical results indicated that the concentration of SiO_2 is the highest of all the elements and ranges from 46.82 to 65.79% with sample T7 which has the highest SiO_2 concentration (65.79%). It is followed by Al_2O_3 (15.25 to 20.13%), Fe_2O_3 (iron has a very high percentage within the specimens of these materials) which varies from 3.71 to 5.23%, K_2O (1.66 – 2.62) and TiO_2 (1.01- 1.30). T1 has the highest concentration of TiO_2 (1.30%). Except for MgO with a value of 1.2% in T6, all the remaining elements have lower values (0.3 – 0.95%). The lowest values are recorded for MnO with concentrations ranging from 0.03 to 0.06. The amount of water is expressed by loss on ignition which ranges from 9.81 to 23.15 wt % for samples T7 and T6, respectively.

Table 3. Chemical composition of the clay materials of the T1, T2, T6 and T7 samples in weight percentages

Samples / Oxides	Elemental concentration (in weight percentages)			
	T1	T2	T6	T7
SiO_2	61.13	57.79	46.82	65.79
Al_2O_3	17.01	15.25	20.13	16.19
Fe_2O_3	5.00	4.63	5.23	3.71
K_2O	2.62	1.83	1.66	2.37
TiO_2	1.30	1.01	1.11	1.09
MgO	0.83	0.89	1.2	0.95
CaO	0.15	0.46	0.36	0.24
Na_2O	0.10	0.07	0.19	0,32
P_2O_5	0.10	0.07	0.09	0.1
MnO	0.03	0.07	0.06	0.03
LOI	11.44	17.69	23.15	9.81
Total	100.00	99.99	100.00	100.00

LOI = loss on ignition

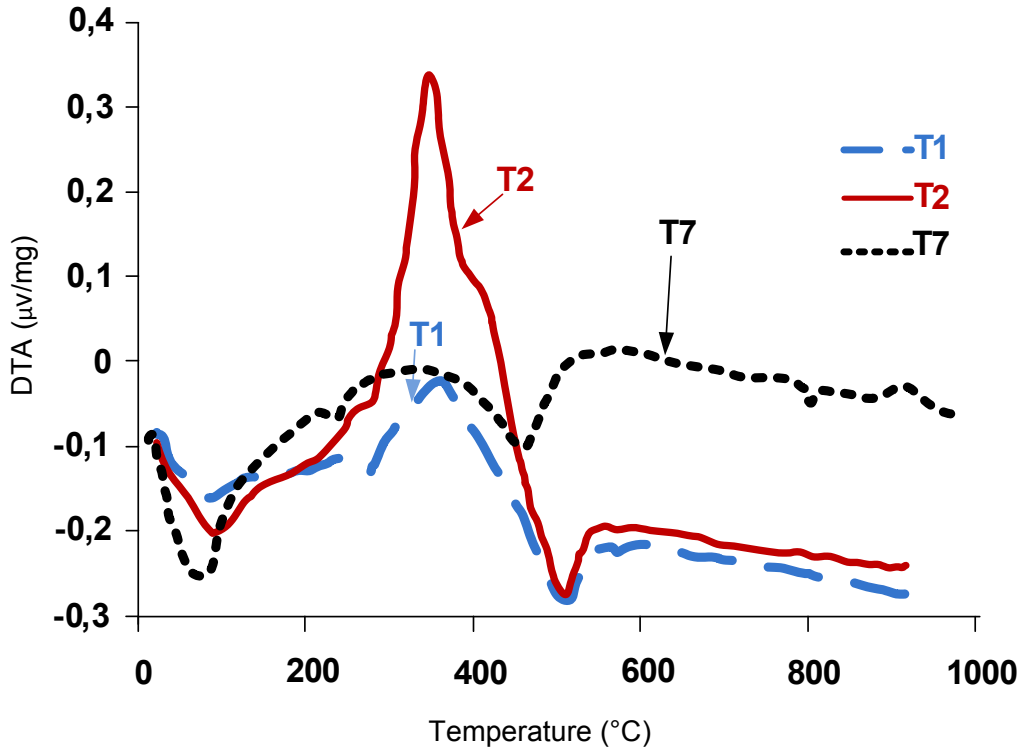

Fig. 6. Differential thermal analysis curves for samples T1, T2 and T7

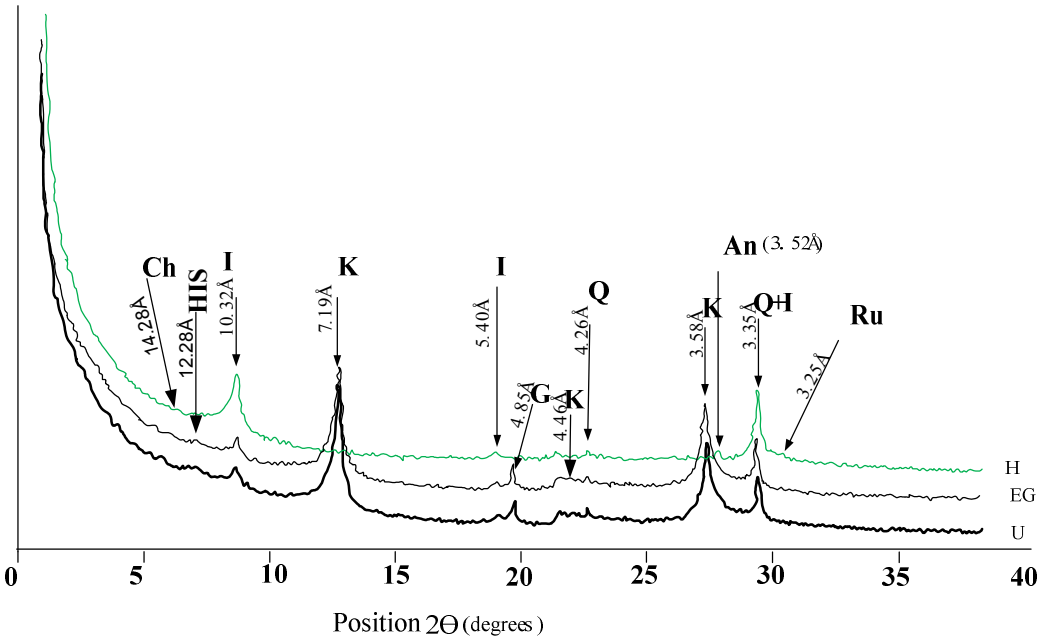

Fig. 7. X-ray diffractograms in < 80 µm fraction of sample T1

U: untreated sample; EG: solvated with ethylene glycol; H: heated at 550°C; I: illite; K: kaolinite; G: gibbsite; Q: quartz; An: anatase; Ru: rutile; Ch: chlorite; HIS: hydroxy-interlayered Na-smectite

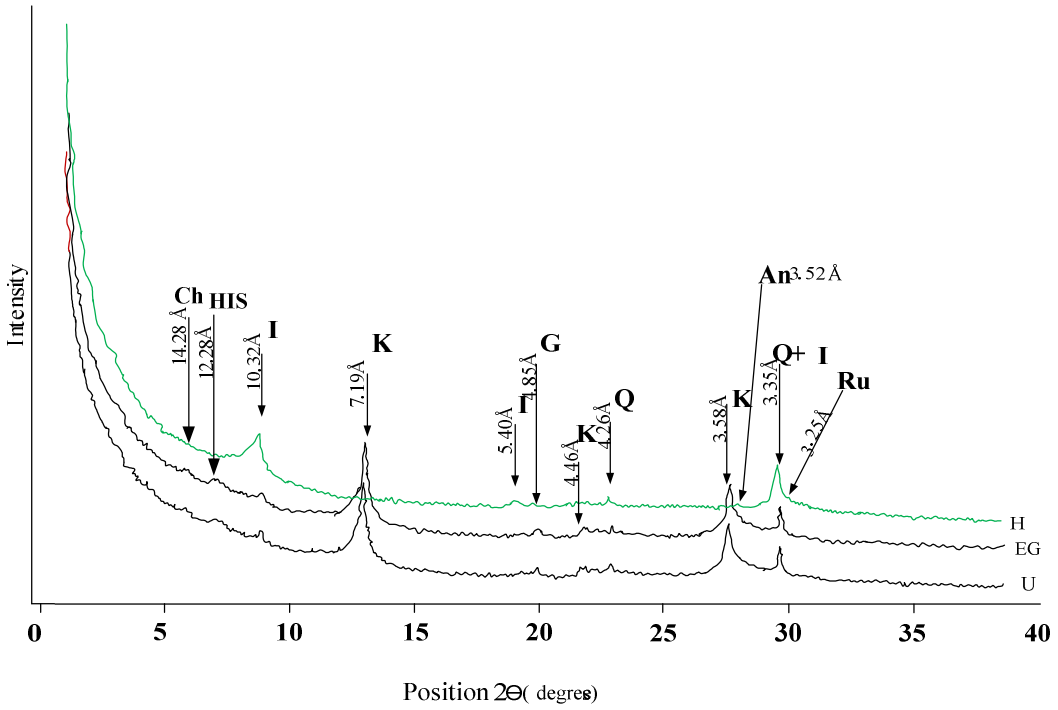

Fig. 8. X-ray diffractograms in < 80 µm fraction of sample T2

U: untreated sample; EG: solvated with ethylene glycol; H: heated at 550°C; I: illite; K: kaolinite; G: gibbsite; Q: quartz; An: anatase; Ru: rutile; Ch: chlorite; HIS: hydroxy-interlayered Na-smectite

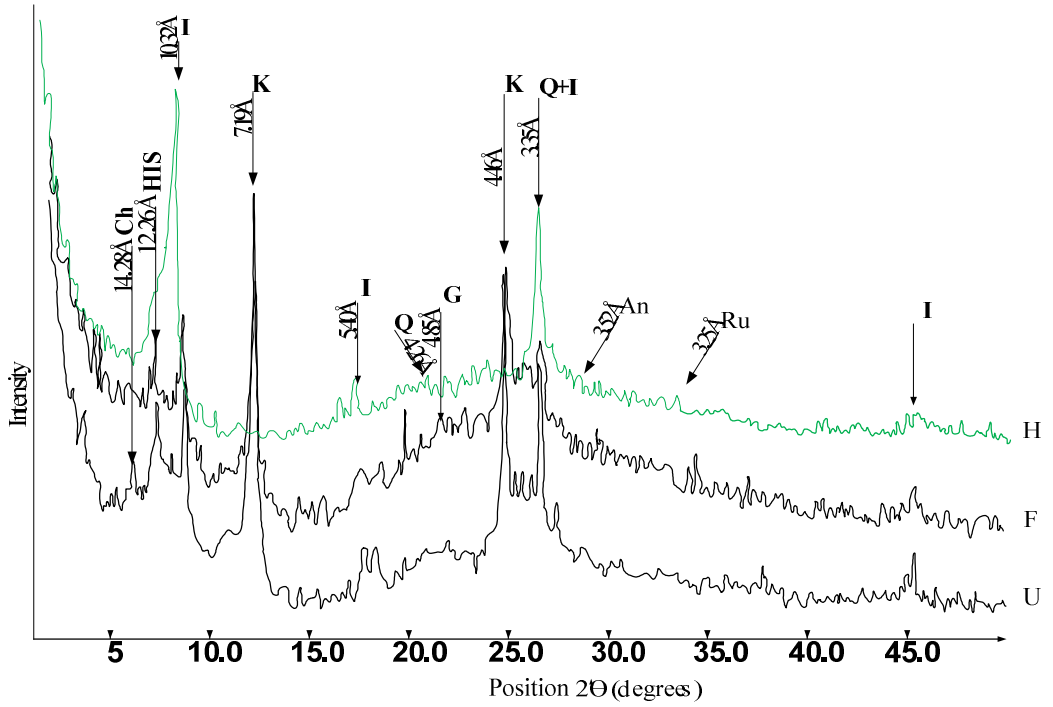

Fig. 9. X-ray diffractograms in< 2 µm fraction of sample T6

U: Untreated sample; F: Solvated with Formamide; H: Heated at 500°C; I: illite; K: kaolinite; G: gibbsite; Q: quartz; An: anatase; Ru: rutile; Ch: chlorite; HIS: hydroxy-interlayered Na-smectite

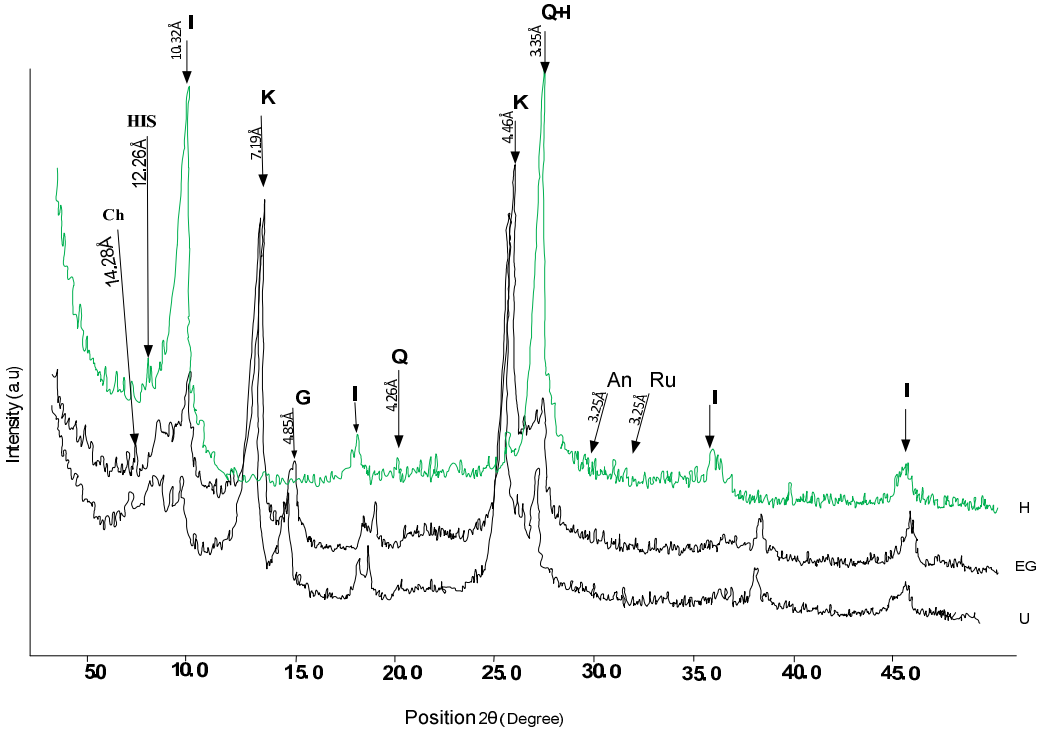

Fig. 10. X-ray diffractograms in < 2 µm fraction of sample T7

U: Untreated sample; F: Solvated with Formamide; H: Heated at 500°C; I: illite; K: kaolinite; G: gibbsite; Q: quartz; An: anatase; Ru: rutile; Ch: chlorite; HIS: hydroxy-interlayered Na-smectite

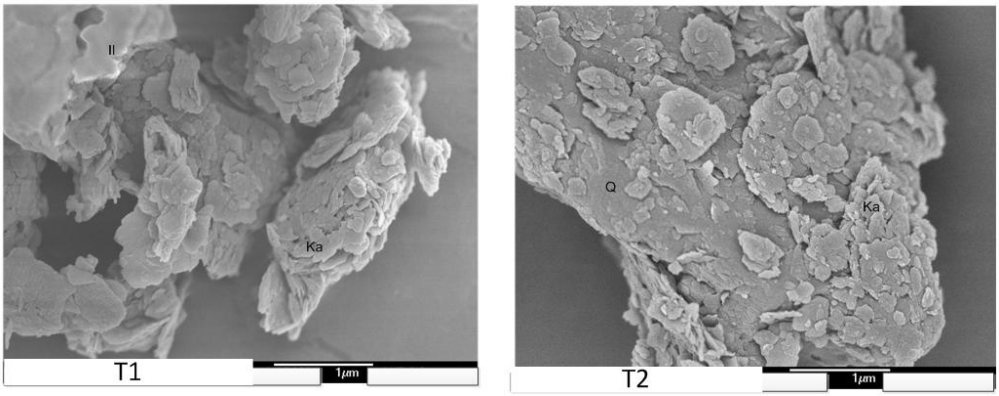

a) Photo 3 b) Photo 4

Fig. 11. Microphotography of the SEM of clay materials of Bamessing

T1 (Clayeys phases pile of kaolinite and illite with irregular form and disorganisation T1 samples) and T2 (SEM image of raw clayeys T2 sample). Ka: kaolinite; II: illite; Q; quartz

5. DISCUSSION

5.1 Field Analyses

The Cameroon Line is a succession of horts and grabbens with a width of about 100 km, stretching in a direction of 30° North [21]. This continental structure belongs to the inter-tropical domain. Generally, it is marked by the development of a thick weathering mantle resulting from surface transformation of rocks of the lithosphere, under the influence of tropical climatic conditions [22]. This transformation led to the production of rock materials, which is

through erosion transported and deposited in the lower zones (sedimentary basins) in the form of sedimentary deposits. This is the case of our area of study which is partly located on a horts and a grabben, with volcanic rocks at high altitudes and the alluvial material at low altitudes. This morphostructural organization is due to the presence of numerous fractures through which the observed watercourses circulate in the South-eastern part of the Bamenda mountains (area of the present study). This fracturing is probably linked to the tectonic episodes responsible for the formation of the Bamenda mountains [23]. The materials observed and described in the profiles of the wells can be grouped into two categories namely: the non-productive layer (non-profitable or not used by craftsmen) and the productive layer (level 3, used by the craftsmen), which is similar to the alluvial clay from Yaounde [24]. The unproductive layer is on the surface, very poor in clay and contains nonweathered rock fragments (volcanics, plutonics and metamorphics), with many roots. This unproductive layer is represented by level I earlier described in the different profiles being similar to the soils developed from the alluvium.

The productive layer, which occurs close to the hydromorphic soils, extends from the surface towards the bottom, but progressively disappears towards the foot of the mountain at the centre of the plain. It is covered by a non-productive layer. This layer has an acid pH, it is rich in kaolinite and has small amounts of illite and also base little amount of quartz which is using in ceramics (20 – 60 µm), but with a lot of quartz grains exceeding 100 µm in size. There is a pancity of feldspars and considerable amounts of oxyhydroxides (goethite, gibbsite).

The productive layer includes levels II and III described in the different profiles. This productive layer contains layers of sand with a lower thickness as that of the quite sticky and plastic clay materials that occur in the humid state in level III. Local population uses the materials from level III for pottery production. The boundaries between these layers are irregular and distinct. The thickness of this layer was not measured because the ground water table occurs above it, thus preventing any further movement. In one of the quarries exploited by crafts men, this layer is reported to be more than twelve meters thick during the dry season.

5.2 Thermo Gravimetric Analysis (TGA)

The weight loss for samples T1, T2 and T7 (11.44%, 17.69%, and 9.81%, respectively) constitute the total amounts of water lost during heating at 999.8°C. The first decreases in weight fall between 22°C and 307°C correspond to the weight loss due to dehydration. The weight decreases of these are around 3.54% for T1 and then vary between 5.61 and 8.54%, presuming the existence of hydrated species in the latter.

The other slopes (between 300 and 1000°C) reveal the dehydroxylation of silicate layers whereby the hydroxides are eliminated from the mineral structure in two steps. This behavior is probably associated with the presence of 1:1 and 2:1 layer silicate and associated interstratified minerals [25]. After 700°C, the loss in weight evolves in a progressive manner up to 999.8°C with a brief sharp drop around 824.8°C. This phenomenon indicates the end of the dehydroxylation of clay minerals of the 2:1 type (muscovite, illite, smectite) and/or the escape of OH^- ions from metakaoline [26]. These phenomena are reported to occur from the surface towards the interior of minerals [27].

5.3 Differential Thermal Analyses (DTA)

The different endothermic and exothermic peaks observed on the DTA curves (Fig. 8) of T1, T2 and T7 represent the dehydroxylation and recrystallization of materials (hydroxyl or oxides, clay mineral and amorphous oxide or silicate) found in the samples. The clayey materials loose the adsorbed and/or inter-layer water between 25 and 250°C [18]. However, the peaks observed between 25 and 100°C (74.89°C, 67.05°C and 76.7°C for T1, T2 and T7, respectively), and 130 and 250°C (178.44°C and 171°C, 3.56°C for T1 and T2, respectively) correspond to the starting water adsorbed of kaolinite and clay minerals of the 2:1 type [28-30]. The third endothermic peak of T1, T2 and T7 at 259.47°C, 264.1°C and 253.1°C respectively, represent a dehydroxylation of gibbsite and goethite layers [31-33]. The DTA curves of T1 and T2 have exothermic peaks at 339.03°C and 350.57°C, respectively. These exothermic peaks correspond to the crystallization of anatase and other oxides of iron, aluminium and titanium or to the presence of amorphous silicates and oxides [34]. The endothermic peaks observed between 470 and 650°C (477.6°C, 498.25°C and 503.63°C), are characteristic of kaolinite

dehydroxylation [1,30,34]. Little depression that appears around 557.41°C is characteristic for 2:1 clay mineral dehydroxylation [1,30,34]. This holds true for the peaks of T1, T2 and T7 at 557.41, 553.63 and 567°C, respectively. The micro-peaks (T7) observed around 824.8°C are due to the slight endothermic phenomena associated with the segregation of domains (2:1 clay mineral) rich in aluminium [35,36].

The mullitisation process is well represented on the T7 curve by the peak with a maximum temperature of 941.1°C. This peak corresponds to the transformation of kaolinite [37]. Two endothermic and exothermic micro-peaks are also observed on this curve, with maximum temperatures of 567°C and 705°C, respectively. The exothermic micro-peaks at 705°C indicate crystallisation reactions (freezing of Fe, Al) under high thermal effects [18]. The three endothermic peaks at 253.1°C, 259.47°C and 264.105°C correspond to the onset of the loss of heating. These phenomena are less sensitive on the DTA curves and are at the origin of the loss of water of oxyhydroxides (goethite, gibbsite). The endothermic peaks at 477.6°C, 498.25°C and 503.63°C have their equivalences on the DTA curve between 377°C and 550°C.

5.4 Mineralogy

5.4.1 Qualitative mineral composition of materials

Certain peaks (Figs. 10 to 12) were observed on the untreated diffractograms (d (001) =12.26 Å). According to [38-40], d (001) values at 2Θ = 8.2º ranging from 12.26 Å should indicated a Na-smectite, but Bamessing material after treatment with glycol ethylene (d (001) = 12.48 Å), they are not fully expand and their crystal structure collapses as indicated by the shift in the 001 peack towards 10 Å after heating at 500 and 550°C in Bamessing materials (Figs. 7 to 10). These peaks occur at 8,2 Å represent hydroxy-interlayered smectite (HIS) with [41,42]. The no fully expansion with glycolated of 2Θ equal to 8.2° or low angle peak and 2Θ equal 25.8° (Figs. 9 to 10) indicated that these peaks are not an interstratified illite/smectite [43], but confirm the presence of hydroxy-interlayered smectite. Feldspars, usually present in the primary clayey materials as residues of decomposition of parent materials [44], exist in trace amounts as indicated by the peaks at 2Θ equal to 20° and 27.95°.

Chlorite which characterised by peak at 2 Θ = 6º corresponding to d (001) = 14.28 Å is not expending with glycolated (characteristic of hydroxyl-interlayered mineral).

Kaolinite has peaks with the highest intensity. The intensity of the peaks indicates the relative magnitude kaolinite>illite> quartz and > associated minerals (gibbsite, goethite, chlorite and hydroxyl-interlayered smectite). From the relative quantification made by XRD Eva software and the relative intensities of the peaks it can be inferred that, kaolinite, illite and quartz are very abundant in Bamessing raw materials. Goethite and gibbsite occurs in small quantities. The feldspar peaks were not detectable in analysed XRD patterns (Figs. 7, 8, 9 and 10). This confirms the lack of feldspar in the material analysed. Phophorous has a low content in specimens, ranging between 0.07 to 0.10%. This mineral has been reported to occur in association with dickite, a crystalline variety close to the kaolinite group [40,45]. The absence of feldspar is the cause of the permeability and roughness of ceramic objects manufactured by the population of Bamessing, for it is the fundamental mineral of ceramic mixture with the role of blending and filling the pores in the course of baking. Had it not been for the absence of feldspars within this kaolinitic clay, these materials should have been of better quality for pottery.

5.4.2 Quantitative mineral composition

From the XRD results, the major crystalline phases contained in all the samples are as follows:

- Illite(I) : $(K,H_3O)Al_2Si_3AlO_{10}(OH)_2$; Kaolinite(K) : $Al_2Si_2O_5(OH)_2$; chlorite:$(Mg_5Fe)Isi_3Al)O_{10}(OH)_8$; hydroxyl-interlayered Na-smectite (HIS): $Na_{0.5}Al_2(Si_{3.5}Al_{0.5})O_{10}(OH)_2n(H_2O)$; Quartz(Q) : SiO_2; Goethite (Go) :FeO(OH) ; Gibbsite (G): AlO(OH); Anatase : TiO_2.

In comparing the results of mineral analyses with those of total chemical analyses, one can proceed by calculation to a quantification of crystalline phases detected in the specimens. Quantitative mineral assessment was done using the mineral calculations method of [6,46] with the following formula: T (a) = ΣMiPi (a). Where: T(a) is the oxide content in percentage in chemical element « a » ; Mi is the mineral content (%) « i » in the material studied and containing the element« i »; Pi(a) is the proportion of the

element « a » in the mineral « i » (this proportion is deducted from the ideal formula attributed to the mineral « i »).

Taking into account XRD patterns of samples (Figs. 7, 8, 9 and 10) and quantitative mineral composition (Table 4), all samples (T1, T2, T6 and T7) contain same mixture of clay minerals with different intensity of peaks: illite, kaolinite, chlorite and hydroxyl-interlayered Na-smectite (Figs. 7, 8, 9 and 10; Table 4). Mixture of clay minerals is estimated in T1 sample at 40.3%, in T2 sample at 35.05%, T6 sample at 46.71% and T7 sample at 38.61%. In quantity illite is higher in T1 sample (22.16%) and less in T6 sample (14.04%), kaolinite higher in T6 sample (24.42%) and less T7 sample (7.77%). Higher percentage of hydroxyl-interlayered Na-smectite and chlorite are respectively in T7 sample (8.04%) and T6 sample (3.48) with less quantity in T2 sample (1.76%) and T1 sample (2.40%). Concerning associate clay minerals, Bamessing has quartz, goethite, gibbsite and anatase. In quantity associate clay mineral is estimated at 49.51%, 46.73%, 30.47% and 51.86% respectively in T1, T2, T6, and T7 sample. With quartz less quantity is in T6 sample (24.61%) and higher quantity in T7 sample (47.44%). Taking into account mineralogical and chemical association (*5.4.1* and *5.4.2*) clayey materials from Bamessing were suitable for ceramic applications. Illite and hydroxyl-interlayered Na-smectite may promote the glassy phase responsible for the densification of the final product [47,48]. Kaolinite (as alkali-free clay) may promote mullite formation (observed in DTA curve).

Table 4. Mineral compositions (percentage) of samplesT1, T2, T7 and T6

Samples / Minerals	T1	T2	T6	T7
Illite (%)	22.16	15.48	14.04	20.05
Kaolinite (%)	16.23	15.22	24.42	7.77
HIS (%)	2.51	1.76	4.77	8.04
Chlorite (%)	2.40	2.58	3.48	2.75
Quartz (%)	42.53	41.44	24.41	47.44
Anatase (%)	1.09	1.3	1.012	1.11
Gibbsite (%)	0.74	0.74	0.73	0.73
Goethite (%)	3.94	3.54	4.02	2.60
Total	**88.82**	**81.78**	**77.20**	**90.47**

5.4.3 Chemical composition of the materials

The loss on ignition (9.81 to. 23.15%) of these samples (T1, T2, T6 and T7) is associated with the presence of clay minerals, hydroxides and organic matter [49]. The presence of considerable amounts of TiO_2 within these materials is characteristic of potassium rocks (lavas) of cratonic environments [50].

The basic components (Alkalis [K_2O Na_2O] and the earth-alkalis [MgO and CaO]) have values below 4%. This accounts for the great plasticity of the clayey materials of Bamessing [51]. Consistent with our findings in [37,52], who reported respectively that clays with a somewhat extensive vitrification is expected since the ratio (K_2O + Na_2O)/(MgO + CaO) approximates 1 (whereas a quantitative melt should be formed for R>1) and low Al_2O_3 contents (Al_2O_3 < 30wt % in oxide form) are non- refractory [53]. The Al_2O_3 contents of all the Bamessing clays materials (< 30 wt %) and the ratio (K_2O + Na_2O) / (MgO + CaO) (2.77 in T1, 1.4 in T2, 1.18 in T6 and 2.66 in T7) is meaning that Bamessing raw material is suitable for porous ceramic products.

6. CONCLUSION

The clay materials of Bamessing lie directly on the Panafrican pedestal. They are surrounded in places by cover rocks (volcanic rocks, Panafrican pedestal) and lateritic soils. Mineral and chemical analysis of clay minerals from levels II and III of Bamessing, using XRD spectrometry, X-ray Fluorescence, DTA, GTA and SEM show that the mineral obtained of the Clayey materials from level II of Bamessing (<200 µm) is composed of: kaolinite, illite, chlorite, hydroxyl-interlayered Na-smectite (HIS), quartz, goethite, gibbsite and poorly crystalline minerals. Clay materials from level III of Bamessing contain the same mineral in quality put as those from level II but different in quantity. Bamessing clayey material (<200 µm) have mixture of clay minerals between 35.05 and 46.71% and associate clay mineral between 30.47 and 51.86%. Its ratio ((K_2O + Na_2O) / (MgO + CaO)) is between1.18 and 2.77. Quantitative mineralogical results of the raw material confirmed that quartz, illite, and kaolinite are the major minerals present with significant amount of hydroxyl-interlayered Na-smectite and chlorite. Illitic sample (T1, T2 and T7 samples) with their chemical properties is generally suitable for various red ceramic bodies. Kaolinitic sample (T6 sample) is suitable for stoneware. Further applied tests on the clays studied have to be carried out to determine the formulations for some red ceramic products.

ACKNOWLEDGEMENT

The authors are very express to thanks to the professor Nguetkam of the University of Ngaoundere Cameroon and the Head of the laboratory of Mineralogy University of Limoges French for the X-Ray diffraction analysis and SEM. The authors are thankful the Head of the Science of Earth and Planetary Materials Laboratory of the Department of Earth and Planetary System Science, Faculty of Science, in Hiroshima University, Japan for the X-Ray diffraction, SEM analysis and chemical analysis.

COMPETING INTERESTS

Authors have declared that no competing interests exist.

REFERENCES

1. Carty M, Senaparti U. Porcelain–raw materials, processing, phase evolution and mechanical behaviour. J. AM. Cera. Soc. 1988;81(1):3-20.
2. Dorlot JM, Bailon JP, Masounave J. Des matériaux. Ecole polytechnique de Montréal. 1980;467. (French)
3. Olivier JF. Agilotherapie : les argiles et leurs compléments naturels, *Edition* Encre/Arys, Paris.1988;194. (French).
4. Caillere S, Henin S, Rautureau M. Les argiles. Ed SEPTIMa, Paris. 1989;126. (French).
5. Kühnel RA. The modern days of clays. Applied Clay Science. 1990;5:135-143.
6. Njopwouo D. Minéralogie et physico-chimie des argiles de Bomkoul et de Balengou. (Cameroun). Utilisation dans la polymérisation du styrène et dans le renforcement du caoutchouc naturel. Thèse Doct. Univ. Yaoundé, Cameroun. 1984;300. (French).
7. Roskill. The economics of kaolin 9th ed., London. 1996;320.
8. Ekosse G. The Makoro kaolin deposit Southeastern Botswana: its genesis and possible industrial application. Applied Clay Science. 2000;16:301-320.
9. Njopwouo D, Tejiogap E, Sondag F, Vollkoff B. Wandji R. Caractérisation mineralogique et chimique des argiles kaolinitiques consommés par geophagisme au cameroun, Annales Fac. Sci. Univ de Yaoundé I Série Math-Info-Phys-Chimie. 1998;31(2):319-334. (French).
10. Tchounang Kouonang S. Prospection et caracterisation physico-chimique des matériaux argileux de Bamessing exploités pour la poterie. Thèse de Master. Univ. Dschang. 2006;79. (French).
11. Toteu SF, Van Schmus WR, Penaye J, Michard A. New U-Pb and Sm-Nd data from north Cameroon and its bearing on the pre-Pan Africa. Precamb. Res. 2001;108:45-73.
12. Kamgang P. Pétrologie et géochimie d'un secteur clé de la ligne du Cameroun, les monts Bamenda; Implication sur la genèse et l'évolution des magmas. Thèse de Doct. D'Etat, Univ. Yaoundé I, Cameroun. 2003;373. (French).
13. Nzolang C, Kagami H, Nenti JP. Holtz F. Geochemistry and preliminary Sr-Nd isotopic data on the Neoproterozoic granitoids from the Bantoum area, West Cameroon: Evidence for a derivation from a Paleoproterozoic to Archean crust, Polar Geosciences. 2003;16:196-226.
14. Kwekam M. Genèse et évolution des granitoïdes calco-alcalins autour de la tectonique panafricaine : le cas du massif desyn à tardi-tectoniques de l'Ouest-Cameroun (région de Dschang et de Kékem). Thèse de Doct. d'Etat. Univ. Yaoundé I. 2005:194. (French).
15. Kamgang P, Chazot G, Njonfang E, Tchoua F. Geochemistry and geochronology of felsic rocks of mount Bamenda NW-Cameroon (line of Cameroon). C. R. Geoscience. 2007; 339:659-666.
16. Kamgang P, Chazot G, Njonfang E, Tchoua F. Geochemistry and geochronology of mafic rocks from Bamenda Mountain (Cameroon): Source composition and crustal contamination along the Cameroon Volcanic Line. C. R Geoscience. 2008;340:850-857.
17. Kamgang P, Njonfang E, Nono A, Gountie DM, Tchoua MF. Petrogenesis of a silisic magma system: Geochemical evidence from Bamenda Mountains, NW Cameroon Volcanic Line. Journal of African Earth Sciences. 2010;58:285-304.
18. Marc P, Jacques G. L'analyse du sol minéralogique, organique et minérale, Springer- Verlag. France. 2003;243. (French).

19. Kitagawa R, Koster HM, Zaikov VV, Udachim VN. Scanning electron microscope examination of quartz surface textures from kaolinized granitic rocks. Journal of Science of Hiroshima University. 1994;10:159-172.
20. Wilson P. A scanning electron microscope examination of quartz grains surface textures from the weathered millstone grit (carboniferous) of the Southern Pennins, England. A Priliminary Report. 1995;319-328.
21. Tchoua FM. Contribution à l'étude géologique et pétrologique de quelques volcans de la ligne du Cameroun (Monts Manengouba et Bambouto). Thèse Doct. D'Etat Univ. Clemont Ferrand. 1974;346. (French).
22. Ekodeck GE, Kamgang KB. L'altérologie normative et ses applications: Une expression particulière de la pétrologie des roches aluminosilicatées du point de vue de leur évolution supergène. Coll. connaissance de press. Univ. Yaoundé. 2002;231. (French).
23. Dongmo JL. Le dynamisme Bamiléké (Cameroun). Volume I : la maitrise de l'espace agraire. Ouvrage publié avec le concours de la Imprimé au CEPER-Ydé. 1982;424. (French)
24. Ngon Ngon GF, Yongue FR, Bonnet JP, Bilong P, Lecomte G. Etude de quelques propriétés physiques et mécaniques de deux argiles kaoliniques de la région de Yaoundé (Cameroun). Sil. Ind. 2005;70:12:174-180. (French).
25. Thiry M, Hauff P. Kaolinite/smectite clay models using thermal and X-ray diffraction data. Proc 7th Euroclay Conf. Dresden'91, Greifswald. 1991;1073-1077.
26. Gualtieri A, Bellottom M, Artiolig G, Clark SM. Kinectic study of the kaolinite-mullite reaction sequence. Part II: mullite formation, Phys. Chem. Minerals. 1995;22:215-222.
27. Bellottom M, Gualtieri A, Artiolig G. Clark SM. Kinetic study of the kaolinite –mullite reaction sequence. Part I: Kaolinite dehydroxylation. Phys. Chem. Miner. 1995;22:207-214.
28. Vionovitch IA. L'analyse minéralogique des sols argileux, Editions Egrolles. 1971;50. (French).
29. Worrall WE. Clays and ceramic raw materials second edition, Elsevier applied Science publishers. 1986;191.
30. Sigg J. Les produits de terre cuites. Septina, Paris. 1991;423. (French).
31. Klimesch DS, Ray A. The use of DTA/TGA to study effects of ground quartz with different surface areas in autoclaved cement: quartz pastes. Use of the semi-isothermal thermogravitric technique. Thermochimica Acta. 1997;306:159-165.
32. Njopwouo D, Kong S. Minéralogie de la fraction fine des matériaux argileux de Bomkoul et de Balengou (Cameroun). Annales de la faculté des Sciences, série des Sciences chimiques. 1986;1(2):17-31.
33. Mohamed H, Salah K, Mohamed B. Mineralogy and firing characteristics of a clay from the valley of Ourika (Morocco). Applied Clay Science. 2002;21:203–212.
34. Lecomte GNNK. Transformation thermiques, organisation structurales et filtrage des composés kaolinite-muscovite. Thèse Doct. Univ. Limoges, Frances. 2004;198. (French).
35. Ikaya. Fiche technique, Centre de traitement et usine. Salé, Maroc. 2004;4. (French).
36. Lemaitre J, Leonard AJ, Delmon B. The sequence of phases in 900-1050°C, transformation of metakaolinite. Proc. Int. Clay Conf. 1997;60(1-2):37-43.
37. Olivier C. Influence de la vitesse du traitement thermique sur le comportement d'un kaolin : application au frittage rapide. Thèse, Université de Limoges. 2000;139. (French).
38. Grim RE. Clay Minerallogy. Mc Graw-Hill book Co. Inc., New York. 1968;596.
39. Yildiz A, Kuseu M. Mineralogy, chemistry and physical properties of bentonites from Baören, Kütahya, W. Anatolia, Turkey. Clay Minerals. 2007;42:399-414.
40. Moore, Duane M, Reynolds Jr, Robert C. X-ray diffraction and the identification and analysis of clay minerals. Oxford University Press, Oxford. 1989;332.
41. Meunier A. Soil hydroxy-interlayered minerals: Are interpretation of their crystallochemical properties. Clays and Clay Minerals. 2007;55:380-388.
42. Ransom MD, Bigham JM, Smeck NE, Jaynes WF. Transitional vermiculite-smectite phases in aqualfs of southwestern Ohio. Soil Science Society of America Journal. 1988;52:873-880.
43. Changling H, Makovicky E, Bjarne Osbaeck. Thermical stability and pozzolanic activity of raw and calcined

mixed-layer mica/smectite. Applied Clay Science. 2000;17:141-161.

44. Shaw JN, Hajek BF, Beck JM. Highly weathered mineralogy of select soils from southeastern U.S. coastal plain and piedmont landscapes. Geoderma. 2010; 154:447-456.
45. Brinley GW, Porter RD. Occurrence of dickite in Jamaica – ordered and disordered varieties. Am. Miner. 1978; 63:554-562.
46. Yvon J, Lietard O, Case JM. Minéralogie des argiles kaolinitiques des charentes. Bull. Minéral. 1982;105:431-437. (French).
47. Castelein O, Soulestin B, Bonnet JP, Blanchart P. Influence of the heating rate on the thermal behavior and the mullite formation from a kaolin raw material, Ceram. Inter. 2000;22-28.
48. Gallagher PK, Brown ME, Kemp RB. In: Brown, M.E., Gallagher, P.K. (Eds.), Handbook of Thermal Analysis and Calorimetry: Applications inorganic and Miscellaneous materials. Elsevier; 2003.
49. Baccour H, Medhioub M, Jamoussi F.and Mhiri T. Influence of firing temperature on the ceramic properties of Triassic clays from Tunisia. J. Mater. Process. Technol. 2009;209:2812-2817.
50. Cundari A. Petrogenesis of leucite bearing lavas in the Roman volcanic region, Italy. The sabatini lavas. Contr. Miner. Petrol. 1979;77:9-21.
51. Ferd, Lietti SA. Guide de la céramique, Normes et caractéristiques techniques, Sion and Monthey, Suisse. 2004;11. (French).
52. Segard G. Study of clays extension in a flame. Doctorate Thesis Technical Science. University of Lille, French. 1980;75 (in French).
53. Alviset L. Matériaux de terre cuite. Techniques de l'ingénieur. 1994;25. (French).

Peer-review history:
The peer review history for this paper can be accessed here:
http://www.sciencedomain.org/review-history.php?iid=1136&id=5&aid=9158